

Yu Xueying (Orcid ID: 0000-0002-9380-5136)
Millet Dylan B. (Orcid ID: 0000-0003-3076-125X)
Wells Kelley C. (Orcid ID: 0000-0003-3025-6878)
Griffis Timothy J. (Orcid ID: 0000-0002-2111-5144)
Baker John M (Orcid ID: 0000-0002-7937-9839)
Gvakharia Alexander (Orcid ID: 0000-0003-1260-4744)
Kort Eric A. (Orcid ID: 0000-0003-4940-7541)
Wood Jeffrey David (Orcid ID: 0000-0001-6422-2882)

Top-down constraints on methane point source emissions from animal agriculture and waste based on new airborne measurements in the US Upper Midwest

Xueying Yu¹, Dylan B. Millet^{*1}, Kelley C. Wells¹, Timothy J. Griffis¹, Xin Chen¹, John M. Baker^{1,2}, Stephen A. Conley³, Mackenzie L. Smith³, Alexander Gvakharia⁴, Eric A. Kort⁴, Genevieve Plant⁴, and Jeffrey D. Wood⁵

¹Department of Soil, Water, and Climate, University of Minnesota, Saint Paul, Minnesota 55108, United States

²Agricultural Research Service, US Department of Agriculture, St. Paul, Minnesota 55108, United States

³Scientific Aviation, Inc., Boulder, Colorado 80301, United States

⁴Climate and Space Sciences and Engineering Department, University of Michigan, Ann Arbor, Michigan 48109, United States

⁵School of Natural Resources, University of Missouri, Columbia, Missouri 65211, United States

*Corresponding author: Dylan B. Millet (dbm@umn.edu)

Key Points:

- We used aircraft measurements to quantify methane emissions from key agricultural point sources in the Upper Midwest during three seasons.
- Top-down methane fluxes are consistent with bottom-up values for beef facilities, but reveal a mis-match for dairies and sugar plants.
- These discrepancies point to potential spatial and temporal misattribution of emissions used for atmospheric inverse modeling.

This is the author manuscript accepted for publication and has undergone full peer review but has not been through the copyediting, typesetting, pagination and proofreading process, which may lead to differences between this version and the [Version of Record](#). Please cite this article as doi: [10.1029/2019JG005429](https://doi.org/10.1029/2019JG005429)

Abstract

Agriculture and waste are thought to account for half or more of the US anthropogenic methane source. However, current bottom-up inventories contain inherent uncertainties from extrapolating limited in-situ measurements to larger scales. Here, we employ new airborne methane measurements over the US Corn Belt and Upper Midwest, among the most intensive agricultural regions in the world, to quantify emissions from an array of key agriculture and waste point sources. Nine of the largest concentrated animal feeding operations (CAFOs) in the region and two sugar processing plants were measured, with multiple revisits during summer (08/2017), winter (01/2018), and spring (05-06/2018). We compare the top-down fluxes with state-of-science bottom-up estimates informed by Environmental Protection Agency (EPA) methodology and site-level animal population and management practices. Top-down point source emissions are consistent with bottom-up estimates for beef CAFOs, but moderately lower for dairies (by 37% on average) and significantly lower for sugar plants (by 80% on average). Swine facility results are more variable. The assumed bottom-up seasonality for manure methane emissions is not apparent in the aircraft measurements, which may be due to on-site management factors that are difficult to capture accurately in national-scale inventories. If not properly accounted for, such seasonal disparities could lead to source misattribution in top-down assessments of methane fluxes.

Plain Language Summary

Key agricultural methane sources are quantified using new airborne measurements in the US Corn Belt and Upper Midwest. Measurements spanned multiple seasons and targeted nine of the largest concentrated animal feeding operations in the region along with two sugar processing plants. Comparing with bottom-up estimates informed by EPA methodology and site-level animal and management data, top-down fluxes agree well with bottom-up estimates for beef but are lower for dairies and sugar plants and suggest a possible mismatch in the timing of emissions.

1 Introduction

Agriculture and waste have been estimated to account for ~35% and ~20%, respectively, of the anthropogenic methane (CH_4) source in the contiguous US [Turner *et al.*, 2015]. The US Corn Belt and Upper Midwest is one of the most intensive agricultural regions of the world and is crucial to the overall US methane budget. The area includes >700 million livestock (including ~28 million cattle and a majority of national swine feeding operations), several industrial centers, and extensive natural wetlands [Harun & Ogneva-Himmelberger, 2013; USDA-NASS, 2018]. Here, we present new airborne measurements of point source methane emissions from animal agriculture and waste as part of the Greenhouse Gas Emissions in the Midwest (GEM) study, and apply the aircraft-derived fluxes to evaluate current bottom-up estimates for these sources.

Previous studies have pointed to large uncertainties in the magnitude, distribution, and seasonality of agricultural methane emissions [Hristov *et al.*, 2014; Miller *et al.*, 2014; Miller *et al.*, 2013]. For example, Cui *et al.* [2017] applied airborne measurements over the San Joaquin Valley to infer regional methane sources that were $1.7\times$ the bottom-up estimates, with livestock

accounting for ~75% of the total flux. Hristov et al. [2017] showed that current inventories differed significantly in their spatial allocation of agricultural methane emissions: within the contiguous US, the Emission Database for Global Atmospheric Research v4.2 FT2010 [EDGAR, 2013] and Gridded EPA [Maasakkers et al., 2016] estimates correlated to only $R^2 = 0.1$ and 0.5 for manure and enteric fluxes respectively. Hristov et al. [2017] further developed a county-level emission inventory based on animal population, with some of the largest discrepancies relative to existing inventories occurring over our study region, the Upper Midwest. Furthermore, a recent study based on tall tower measurements in the US Upper Midwest concluded that livestock methane emissions were underestimated 1.8-fold in the Gridded EPA inventory [Chen et al., 2018].

Additional uncertainties in bottom-up inventories can arise from the specification of livestock emission factors (EFs) for enteric fermentation and manure management, as these EFs vary strongly across animal categories, management systems, and climate zones. For example, the recommended enteric EFs for US dairy cattle based on the IPCC Tier 1 method [IPCC, 2006] are 2.4× those for other US cattle, mainly due to differences in feed intake, milk production and other related factors. Manure EFs are even more variable, as they are highly sensitive to management practices and climate conditions. Recommended per-animal manure management EFs in North America thus vary from $<50 \text{ kg y}^{-1} \text{ head}^{-1}$ to $>110 \text{ kg y}^{-1} \text{ head}^{-1}$ in cold versus warm areas, and methane conversion factors (MCFs) for dry manure management systems are typically only ~10% those of liquid systems under similar climate conditions [IPCC, 2006].

Mischaracterization of livestock or of manure management practices can therefore lead to significant errors in national-scale methane emission inventories [IPCC, 2006].

Top-down point source measurements can provide an independent means of i) quantifying point source methane emissions, ii) identifying deficiencies and potential improvements in current emission inventories, and iii) informing source attribution and mitigation planning. In this paper, we apply an airborne mass balance approach for point source quantification to derive top-down constraints on methane emissions from nine of the largest concentrated animal feeding operations (CAFOs) in the US Upper Midwest. Together, the targeted CAFOs include ~105,000 animals, and include five dairies, two beef feedlots and two swine facilities. We also quantify methane emissions from two sugar beet processing plants. These plants are estimated to be among the largest industrial methane point sources in the Upper Midwest, but they represent a methane source category that has received little attention or evaluation to date [eCFR, 2019; GHGRP, 2017].

Facilities were visited multiple times during summer, winter, and spring to assess emission variability within and across seasons. The resulting aircraft-derived fluxes are then compared with state-of-science bottom-up estimates informed by facility-level data to test how well current inventories capture the magnitude and variability of methane emissions from these sources.

2 Data and Methods

2.1 GEM flights and methane point sources

The GEM campaign focuses on understanding methane emissions and related processes in the US Upper Midwest. Flights were conducted by Scientific Aviation Inc. (<http://scientificaviation.com>) on a fixed-wing, single-engine Mooney aircraft (typical boundary layer cruise speed ~280 km/h) with air sampling inlets on the outboard wing section. GEM included 23 flights during summer (GEM-1; 08/2017, 8 flight days), winter (GEM-2; 01/2018, 7 flight days) and spring (GEM-3; 05-06/2018, 8 flight days), with 156 flight hours in total. Flight tracks are illustrated in Figure 1. Along with the point source measurements, GEM also included extensive boundary layer surveying to characterize the distribution of methane and other trace gases across the broader region. Flights were typically 7 hours in duration (between 10am and 7pm local time), and mainly conducted within the atmospheric mixed layer (400-800 m above-ground), with 1-2 vertical profiles per flight extending into the lower free troposphere. All GEM flights were conducted under favorable atmospheric conditions (e.g., suitable mixing depths, sufficient and steady winds; Table S1) in order to mitigate as much as possible the main meteorological sources of uncertainty in the analysis.

The instrument payload included a cavity ring-down spectrometer (Picarro CRDS; model G2301 during GEM-1, model G2210-m during GEM-2/3; Picarro Inc., Santa Clara CA) providing ~1-3-second measurements of methane, ethane (C_2H_6 ; GEM-2 and GEM-3 only), water vapor (H_2O), and carbon dioxide (CO_2); a continuous-wave tunable infrared laser absorption spectrometer (CW-TILDAS, Aerodyne Research Inc., Billerica MA; described in Gvakharia et al. [2018]) providing ~2-second measurements of H_2O , CO_2 , carbon monoxide (CO), and nitrous oxide

(N₂O); and a dual-beam ultraviolet spectrometer (model 205, 2B Technologies Inc., Boulder CO) providing ~5-second ozone (O₃) measurements. Calibrations were performed on the ground for the Picarro CRDS and in-flight for the Aerodyne TILDAS using compressed ambient-level gas cylinders traceable to NOAA Global Monitoring Division standards. Other on-board measurements included temperature and relative humidity (model HMP60, Vaisala Corp., Helsinki Finland), along with location, aircraft speed and direction, pressure, wind speed and direction, and other flight parameters provided by the avionics system and differential Global Positioning System.

A total of 11 major point sources (nine CAFOs + two sugar plants) were quantified during 15 of the GEM flights, with details in Table 1, Table S1 and Figure 1. The targeted facilities were selected based on their estimated methane emission magnitude and accessibility for airborne sampling. The dairies (Table 1) are five of the largest in Minnesota (MN) and together house ~34,000 animals (MN Department of Agriculture (MDA), personal communication). The beef CAFOs are two of the largest such facilities in the region, with >20,000 animals combined (MN Pollution Control Agency (MPCA), personal communication). The swine facilities are two of the largest in MN and Iowa (IA) based on number of animals, with a combined >48,000 hogs (MPCA, personal communication; Iowa Department of Natural Resources [IADNR, 2018]). Finally, we selected two sugar plants for quantification as emblematic examples of this type of operation. According to the US EPA Greenhouse Gas Reporting Program [GHGRP, 2019] 2017 report, the operator of these plants is the largest corporate methane emitter (169,785 metric tons

CO₂ equivalent per year, tCO₂e/y) in North Dakota (ND) and the second largest (302,685 tCO₂e/y) in MN based on their two ND and three MN facilities (the two targeted facilities accounted for an estimated 228,336 tCO₂e/y). For comparison, Continental Resources Inc. reported a methane flux of 178,968 tCO₂e/y in 2017 from their oil + gas operations throughout the Williston basin (including the Bakken Formation), which was the highest of any such operator [GHGRP, 2019].

2.2 Top-down estimation of point source methane emissions

Figure 2 illustrates the aircraft-based point source quantification approach, which is described in detail by Conley et al. [2017] and briefly reviewed here—with additional information in the supporting information. The approach has been successfully used in many recent studies to quantify the magnitude and variability of point source methane emissions [Johnson et al., 2017; Lavoie et al., 2017; Mehrotra et al., 2017; Smith et al., 2017; Vaughn et al., 2017].

The airborne sampling consists of a vertically stacked set of circuits (~1 km radius) around each facility extending from as close to the ground as possible through the extent of the plume. In this work, the vertical sampling typically extended from ~60 m through ~800 m above ground (~300 m for the winter deployment) and included 12-16 individual flight circuits per point source. The total methane emission for a given facility is obtained via summation of the measured advected enhancements as a function of height through the plume, as described in the supporting information. In cases where a point source was quantified more than once in a single season, we use the averaged derived emission as the best top-down estimate.

2.3 Uncertainty in top-down estimation of point source methane emissions

Major factors that can affect the accuracy of aircraft-based point source flux estimates include instrumental uncertainty, weak or variable winds, shallow mixing depths (limiting the number of circuits that can be completed and increasing the extrapolated fraction below the lowest flight leg), and heterogeneity in the methane background [*Gvakharia et al.*, 2017; *Karion et al.*, 2015; *Krings et al.*, 2018; *Mehrotra et al.*, 2017; *Ryoo et al.*, 2019]. Here we estimate the overall top-down flux uncertainty due to these factors from the variance in the measured methane enhancements and the precision of the wind and methane measurements, as described in supporting information. Additionally, we account for uncertainty in the time offset between trace gas and other measurements (wind speed and direction, position, etc.) due to the sampling delay introduced by the ~5 m of ~3 mm OD inlet tubing and by non-zero instrument response time. Application of an incorrect lag time would artificially displace the observed plume from its true downwind location and lead to an emission underestimate. Puff tests performed on the ground revealed a lag time for the methane analyzer of 7-9 seconds. Since the actual in-flight lag time may vary with pressure or other factors, we carry out a sensitivity analysis in which we repeat the calculation for a range of physically realistic lags. This range is defined from the point source measurements themselves, based on the assumption that the true lag time should correspond to the highest computed emissions. In most cases (62%; exceptions have other nearby methane sources), lag times derived in this way range from 6 to 14 seconds. We therefore quantify the lag time uncertainty from the range in emissions calculated across 6-14 second lags, with the best

estimate using a value of 7 seconds (GEM-1) or 8 seconds (GEM-2 and GEM-3) based on the puff tests.

The above uncertainties are then added in quadrature to arrive at the total top-down flux error estimate. In cases where a point source was quantified more than once in a single season, the aggregated uncertainty is defined as the root mean square of the individual errors. Later (in Section 3.5) we discuss the potential for error sources not explicitly accounted for in the above treatment (e.g., temporally variable facility emissions) to affect our results.

2.4 Bottom-up estimation of point source methane emissions

We derived bottom-up flux estimates for each facility for evaluation against the top-down aircraft-based constraints. The bottom-up calculations are based on the current methodologies used in inventories, as described below.

2.4.1 Concentrated animal feeding operation (CAFO) methane emissions

Bottom-up CAFO emissions are calculated from per-animal methane EFs and facility herd size.

The US EPA provides annual state-level methane emission estimates (1990-2015) across 14 animal categories for manure management and across 18 animal categories for enteric fermentation. The US EPA cattle methane emissions are based on EFs derived using IPCC [2006] Tier 2 methods from manure characteristics such as volatile solids content (in the case of manure management emissions) and gross energy intake (in the case of enteric emissions). Swine methane emissions are based on the IPCC [2006] Tier 1 method, which draws from literature

values or from averaged Tier 2 EFs. Here we divide the 2015 state-level emissions by the corresponding animal populations from the United States Department of Agriculture (USDA) [USDA-NASS, 2018] to obtain per-animal manure and enteric EFs by animal category. We employ the EPA ‘dairy cow’ category for dairy cattle, the ‘swine-market’ category for swine ≥ 55 lbs, and the ‘swine-breeding’ category for swine < 55 lbs. In the case of beef CAFOs, we calculate weighted-average EFs for ‘beef-feeding’ and ‘beef-slaughter’ categories (which are those reported by facilities for permitting purposes) based on state-level populations for relevant sub-categories. Uncertainties related to animal categories on-site will be discussed in the Results and Discussion section.

We then multiply the above per-animal EFs by the facility herd sizes to estimate site-level methane emissions. Dairy herd sizes are based on current facility-level data from MDA (personal communication), while beef CAFO herd sizes are based on the facility-reported maximum animal populations by category during 09/2015-08/2016 (MPCA, personal communication). The Swine CAFO A (located in IA) herd size is estimated using permit data from the IADNR. The permit data indicates an animal unit (AU)/head ratio of 0.4, reflecting swine over 55 lbs; swine-market EFs are thus applied in this case. The Swine CAFO B (located in MN) herd size and weight distribution are based on permit data and MPCA site visits; over half (55%) of the reported animals at this facility are < 55 lbs, so that both the swine-breeding and swine-market EFs are applied accordingly.

Seasonal variability in the bottom-up CAFO emission estimates follows Gridded EPA inventory procedures [Maasakkers *et al.*, 2016]. Liquid manure management fluxes are scaled monthly to account for fluctuating temperatures:

$$f = \exp\left[\frac{E_a(T_s - T_0)}{RT_0T_s}\right] \quad (1)$$

Here, the Van't Hoff-Arrhenius factor f quantifies the microbial activity rate at temperature T_s (K) relative to reference temperature T_0 (303.16 K). T_s is the local monthly-mean surface skin temperature obtained from bilinear interpolation of $0.5^\circ \times 0.625^\circ$ gridded data from the Modern-Era Retrospective analysis for Research and Applications Version 2 (MERRA2 [Gelaro *et al.*, 2017]), E_a is the associated activation energy (64 kJ/mol), and R is the ideal gas constant.

Monthly values of f are normalized to their annual mean and used to impose a seasonal cycle on methane emissions from liquid systems. Enteric fermentation and solid manure management emissions are assumed to be non-seasonal. Information on CAFO manure management practices is obtained from facility-level data (beef CAFOs: MPCA, personal communication; Swine CAFO A: IADNR [2018]) or state-level statistics (others: USEPA [2018]).

Uncertainties in the bottom-up enteric fermentation emissions are estimated at 20% for cattle and 30% for swine, following IPCC [2006] recommendations. Manure emission uncertainties are derived from a suite of sensitivity calculations using alternate assumptions for temperature and management practices, as follows. For liquid manure systems, heat from microbial activity typically maintains the lagoon temperature above freezing during winter. Accordingly, the US

EPA recommends a temperature floor of 5 °C (for uncovered anaerobic lagoons) or 7.5 °C (for liquid/slurry and deep pits) [USEPA, 2018]. Other approaches have also been proposed. In particular, Park et al. [2006] derived a linear relationship between manure and air temperature based on year-round measurements from three sites in Ontario, Canada (a cold climate zone). Sensitivity calculations used here therefore include the following. Case 1 sets temperature floors as recommended by the US EPA, with weighting of manure management systems based on facility reports and state-level statistics. Cases 2 and 3 likewise employ the EPA-recommended temperature floor but assume 100% uncovered anaerobic lagoons (Case 2) or 100% liquid/slurry or deep pit systems (Case 3). Cases 4 and 5 follow the temperature relationship from Park et al. [2006], assuming weighted management systems (Case 4) or 100% liquid systems (Case 5). Case 6 assumes 100% dry systems, with no seasonal variation. Our best bottom-up estimates are the mean of Cases 1 and 4, with the uncertainty defined as the range from all six cases. Finally, while population uncertainty is not explicitly included in the above treatment, the herd-size data is obtained from a combination of site visits and permit data—which we assume to be a smaller error source than the other factors discussed above.

2.4.2 Sugar processing plant emissions

Bottom-up emissions for the two targeted sugar plants are based on facility reports for year-2017 [GHGRP, 2019] (while GEM included airborne sampling during both 2017 and 2018, the GHGRP emissions for these facilities differ by <2.5% between the two years). The reported data includes annual methane flux estimates for 1) stationary fuel combustion, and 2) waste + landfill

emissions. We disaggregate the former to monthly values based on fuel usage and assume the latter to be non-seasonal, following the Gridded EPA inventory methodology [Maasakkers *et al.*, 2016]. The reported industrial waste + landfill methane emissions account for >99% of the total, and reflect waste streams from handling and processing of sugar beets and pulp by-products, and from sugar extraction [Dilek *et al.*, 2003]. These waste streams are distributed to a series of holding ponds which can be used for spray irrigation or undergo treatment for discharge to surface waters [SMBSC, 2019]. The resulting emissions reported to the GHGRP are estimated based on the load capacity of the waste system and recommended methane generation rates from the US EPA [GHGRP, 2017]. Bottom-up uncertainties for the above sugar plant emissions are estimated here from the 2011-2018 range in GHGRP-reported values.

3 Results and Discussion

In this section we present the aircraft-based emission estimates for each point source category, assess their degree of consistency with bottom-up estimates, and discuss implications of our findings for bottom-up source estimation. The results of the airborne point source quantifications (performed over 15 days spanning three seasons) are summarized in Table 1 and Figure 3.

3.1 Consistency between top-down and bottom-up total methane emissions for beef concentrated animal feeding operations (CAFOs)

The aircraft-derived fluxes broadly support the bottom-up estimates for beef CAFOs, with a mean top-down:bottom-up ratio of 0.99 (averaged aircraft-based fluxes and bottom-up estimates

have no significant difference at the 95% level based on a paired t -test). As shown in Tables 1, Table S1 and Figure 3 (f-g), the top-down and bottom-up emissions agree to within 60% (difference/mean) in all cases except the Beef CAFO B summer visits, when a larger discrepancy is found (81%). Herd sizes at the two facilities are 10,500-12,000, leading to a mean bottom-up estimate of 66 kg/h per facility for the months with GEM measurements—in good agreement with the mean top-down value of 61 kg/h. The corresponding EF derived from the aircraft measurements is 51 kg y⁻¹ head⁻¹, compared to the bottom-up values of 50 kg y⁻¹ head⁻¹ and 60 kg y⁻¹ head⁻¹ for beef-slaughter and beef-feeding categories, respectively.

We see in Figure 3 that the bottom-up seasonality assumed for beef CAFOs is significantly weaker than in the base-case bottom-up estimate for dairies, and the GEM airborne measurements are generally consistent with this lack of seasonal variation. Nearly all MN beef CAFOs use dry manure management systems [USEPA, 2018], which have an assumed MCF of only 1% that does not vary seasonally. Enteric fermentation is thus the dominant methane source from beef CAFOs in the bottom-up estimates, accounting for >96% of the total emissions. As a result, the bottom-up beef CAFO emissions are only 5% higher in summer than in winter. The airborne methane emissions, while only representing temporal snapshots, are consistent with this picture as they show no clear evidence of a consistent difference in fluxes by season.

3.2 Aircraft-derived methane fluxes over dairies: consistency with bottom-up enteric-only emissions, mismatch for manure

The seasonally averaged best-estimate aircraft-derived fluxes (Tables 1 and S1; Figure 3 a-e) for dairies are lower than the total bottom-up estimates by on average 37%; mean top-down:bottom-up scale factors across facilities span 0.14-0.45, 0.54-0.98, and 0.44-0.77 during summer, winter and spring respectively. Of the 22 site-visits, only two top-down fluxes exceed the bottom-up estimates (by 4%-10%). The dairies quantified each have 6,000-8,000 animals on-site, leading to bottom-up emissions averaging 171 kg/h per facility, and varying with animal population from 147-204 kg/h. In contrast, the airborne measurements imply a mean emission rate for those same periods of 96 kg/h per facility, ranging from 71-129 kg/h (Table 1). On a per-head basis, the GEM flights indicate an average methane EF across the sampled seasons and facilities of 132 kg y⁻¹ head⁻¹, versus 212 kg y⁻¹ head⁻¹ from the EPA inventory [USEPA, 2018] for dairy cow manure + enteric emissions. On the other hand, the aircraft-derived fluxes are consistent with the bottom-up enteric-only methane fluxes, with no statistical difference at the 90% significance level. Consequently, across the sensitivity tests described in Section 2.4.1, the bottom-up estimates agreeing most closely with the aircraft-based fluxes are those with the lowest manure methane emissions. Potential implications of this are discussed later.

The above top-down versus bottom-up total flux differences for dairies vary by season: mean top-down fluxes across facilities are 77% of the bottom-up value in winter, 60% in spring, and only 30% in summer. Figure 3 (a-e) shows that current bottom-up methodologies imply a significant seasonal amplitude in methane emissions from dairies: the base-case inventory-based fluxes for our targeted facilities vary seasonally by ~45% (range/mean) due to the effect of

temperature on predicted manure emissions (manure and enteric emissions make up ~40% and ~60% of the bottom-up flux for these dairies). However, this strong variation is not apparent in the aircraft measurements, which reveal no clear or consistent seasonal differences.

These mismatches in flux magnitude and seasonal pattern are persistent and manifest across all of the individual dairies visited (Figure 3). The results thus point either to some systematic misdiagnosis in our bottom-up estimates, or to a systematic error in the top-down calculations. Some potential explanations for this finding are discussed below.

1) The bottom-up estimates mis-diagnose manure emissions from dairies due to management or other factors that modify the manure emission seasonality and/or magnitude. An overestimate of the manure-related methane source during the timeframes of the GEM flights could explain both the lack of observed seasonality and the bottom-up bias. As shown previously, the bottom-up beef CAFO emissions, which are predominantly enteric, agree well with the aircraft-based fluxes, implying that the cattle enteric source is accurately represented in current inventories.

Conversely, swine facility emissions (see next section), which mainly reflect manure sources, appear to be highly variable based on the aircraft-based fluxes. Our top-down measurements for dairies are consistent (in terms of magnitude and seasonal differences) with the enteric-only bottom-up fluxes (Figure 3), supporting the idea that the manure methane source is the most likely cause of the discrepancy.

Physical mechanisms that could explain this include both environmental and management factors.

For example, the effective temperature dependence of microbial methane production from

manure might be weaker than assumed in our calculations. We use diel-mean surface skin temperature to drive the bottom-up manure emissions. Prior work has shown that manure temperatures can be warmer or cooler than ambient air temperature, and that methane emissions have a lagged response to temperature changes [*Kariyapperuma et al.*, 2018; *Park et al.*, 2006]. However, in situ measurements [*Kariyapperuma et al.*, 2018; *Maldaner et al.*, 2018; *Park et al.*, 2006; *Ulyatt et al.*, 2002] clearly show a seasonal cycle in manure methane emissions, so that in the absence of mitigating factors the same should manifest here for the manure-driven fluxes.

Along with temperature, factors such as pH, humidity and management practices (e.g., lagoon covers, separation of solid from liquid manure for use as bedding) can influence the timing and magnitude of manure-related methane emissions [*Scheutz et al.*, 2009; *VanderZaag et al.*, 2013]. Furthermore, manure at these facilities is typically removed yearly (e.g., in fall) for land application, which may cause on-site manure amounts to vary significantly between seasonal visits. No such effects are accounted for in our bottom-up calculations or in current inventories. Finally, in-flight photographs show that some of the sampled dairies appear to employ synthetic lagoon covers under negative pressure, which can decrease manure methane emissions. Current bottom-up methodology assumes only a 25% reduction in facility-level manure emissions with the use of lagoon covers [*USEPA*, 2018], but the actual reduction may be greater for facilities targeted here.

2) An alternative explanation could be that the seasonality for enteric emissions is incorrectly described in the bottom-up calculations, and in fact offsets the manure emission seasonality.

Previous studies have shown that nutritional changes and other factors can have important effects on enteric methane emissions [*Beauchemin et al.*, 2008; *Boadi et al.*, 2004]. However, to explain the airborne results, the enteric seasonality would have to be phase-shifted relative to the manure source (i.e., be higher in winter). We consider this explanation improbable as such reversed seasonality is not seen in the aircraft-derived beef CAFO emissions (see previous section), which are thought to mainly reflect enteric fluxes.

3) Sparse temporal sampling. Finally, it needs to be emphasized that the aircraft data provides only a snapshot in time, and that sustained measurements are needed to fully characterize seasonal cycles. However, the fact that the same weak seasonal tendencies are seen in the aircraft fluxes for all of the targeted dairies suggests that the factors driving methane variability for these facilities are not well captured in current inventories used in models.

3.3 Highly variable methane emissions from swine facilities

While the bottom-up estimates for the two targeted swine facilities are within 16% (difference/mean), the airborne measurements imply that their actual fluxes differ by $>26\times$ (Tables 1 and S1; Figure 3 h-i), suggesting a large bottom-up underestimate in one case but a large overestimate in the other. The mean aircraft-derived flux is $2.5\times$ the bottom-up estimate for Swine CAFO A (~20,000 animals), but $0.08\times$ the bottom-up value for Swine CAFO B (~29,000 animals) (Table 1). The resulting aircraft-derived EFs are $71 \text{ kg y}^{-1} \text{ head}^{-1}$ (Swine CAFO A) versus only $2 \text{ kg y}^{-1} \text{ head}^{-1}$ (Swine CAFO B). For comparison, the EFs assumed in the bottom-up estimates for the same time periods range from 11-21 $\text{kg y}^{-1} \text{ head}^{-1}$. A possible contributing

factor is the fact that Swine CAFO B houses mostly (55%) smaller animals (<55 lbs) whereas the other one does not—i.e., the bottom-up calculations could underestimate methane emissions for large pigs and overestimate them for small pigs. Given the magnitude of the observed emission difference, however, it seems unlikely that this is the main explanation, and we hypothesize that differing management practices at the two facilities drive the observed disparity. For example, some swine facilities have significant under-barn manure storage, where environmental conditions can differ significantly from outdoors. Facility-to-facility variabilities in such factors likely play a role in the observed flux difference. Furthermore, the repeat aircraft visits to Swine CAFO A point to substantial temporal variability in emissions—which is unexplained and which we are unable to characterize for Swine CAFO B (single visit).

For both targeted swine facilities, manure management is the dominant methane source in the bottom-up calculations, accounting for 91% of the total. Enteric emissions (estimated at 0.01-0.03× those of cattle per animal [*USEPA, 2018*]) account for the remainder. Based on state-level statistics from the US EPA, ≥90% of the swine facilities in this region use liquid manure management systems; as a consequence, the bottom-up fluxes are strongly seasonal, with summertime emissions >4× those during winter (Figure 3 h-i). The GEM flights targeted these facilities only during spring, and thus provide no constraint on this assumed seasonality.

3.4 A large bottom-up overestimate of sugar waste methane emissions

The airborne measurements imply a dramatic (3-14×) overestimate of methane emissions from sugar plants, and a possible underestimate of the associated seasonality (Table 1; Figure 3 j-k).

The bottom-up emissions, based on facility-reported data to the 2017 GHGRP, are on average 472 kg/h for Sugar Plant A and 569 kg/h for Sugar Plant B (>99% from waste) during 2017. In contrast, the aircraft-derived fluxes for Sugar Plant A are only 0.3× the bottom-up values during summer (146 kg/h) and spring (161 kg/h), and 0.1× the bottom-up value during winter (38 kg/h). Sugar Plant B was only visited during winter, but the derived top-down fluxes are very low (41 kg/h) and consistent with those obtained for Sugar Plant A at the same time of the year.

The GEM flights only included a total of four site visits for the sugar plants, and thus cannot fully characterize the seasonality of the associated methane emissions. However, the significantly lower airborne fluxes compared to the bottom-up estimates do suggest that the inventory values are too high, while the 4× higher top-down fluxes derived for summer/spring versus winter call into question the lack of bottom-up seasonality. Current methane emission reports for these types of facilities are highly generic, using default waste decay rates based on regional categories for annual rainfall and the recirculated leachate application rate [*eCFR*, 2019]. In fact, noticeable odors from these facilities typically occur beginning in spring due to i) thawing of the waste ponds that freeze over winter, and ii) thawing and subsequent deterioration of the frozen beet piles being stored for later processing [*ACSC*, 2019]. Rainfall and snowmelt also lead to wastewater seasonality by flushing the waste from stored beets and by modifying the water volume that is transmitted to the holding ponds. Since the resulting seasonal odors reflect microbial decay, methane generation might follow a similar pattern. Revised EFs for sugar waste,

plus an explicit representation of the above seasonal factors, would likely improve the bottom-up emissions for this type of facility.

3.5 Remaining uncertainties

Uncertainties relevant to above findings could arise from vertical extrapolation of the aircraft observations, temporal emission variability, and the assignment of livestock EFs. Below, we discuss each of these in turn and assess their implications for our analysis.

In the case of the top-down estimates, we compute surface layer fluxes based on the average value over the lowest measured vertical layer. We consider this to be the most robust general approach. However, depending on vertical mixing this assumption might misrepresent the surface layer fluxes in some cases (e.g., if the methane plume is confined to the near-surface). An alternate approach is to compute the surface layer fluxes by extrapolating the vertical flux gradient between the two overlying layers to the ground. Using this methodology, the top-down emissions would be $1.2\times$ (median ratio) the current estimates. Overall, while estimation of the flux component below the sampling floor is an important source of uncertainty in the aircraft-based estimates, we find that our core findings are robust to the assumptions used therein.

Additional uncertainties could arise from temporal emission variability that is not captured by the aircraft snapshots. However, Table S1 and Figure 3 show that most facilities were revisited intra-seasonally at least once, providing an opportunity to examine the variability of the airborne flux estimates. All revisits took place within 10 days of each other. During winter, the median

normalized difference (range/average) of the derived fluxes for revisits is 25%, while it is 62% during spring. On just two occasions (one dairy and one beef CAFO) does the normalized difference exceed 100% (102% and 188%, respectively). These larger differences (and the larger spread observed during spring compared to winter) may be due to meteorological factors affecting the accuracy of top-down quantification, but they may also reflect real temporal variance in emissions. While large changes in animal population in such a short time span appear unlikely, other management shifts can alter emissions, such as covering/uncovering of the lagoons, transferring of manure, or its application to fields. For example, when an on-site manure reservoir is emptied, it is often stirred, leading to short-term emission spikes [VanderZaag *et al.*, 2014]. The GEM flights measured 11 facilities over 23 flights. Clearly, more sustained measurements are needed to fully characterize the temporal variability and seasonality of methane emissions from these sources.

In the case of the bottom-up estimates, we rely on two important assumptions in the assignment of livestock EFs. Firstly, we use state-level data to assign livestock categories and manure management practices. Factors such as animal age, weight, diet, and management systems can significantly influence livestock EFs. Thus, state-average versus facility-level differences for the above factors could account for some of the top-down/bottom-up discrepancies inferred here. We assessed some aspects of this uncertainty using a sensitivity analysis across management practices and assumed temperature dependencies, as described previously. However, there are likely other facility-to-facility differences relevant for methane that are difficult to capture

accurately in large-scale inventories, and in the absence of more site-specific information. Secondly, we assume that all cattle present at the dairies fall under the ‘dairy-cow’ category. If some are in fact heifers (i.e. have not produced calves nor therefore milk), the bottom-up emission estimates would be reduced (heifer enteric and manure management EFs are 0.45× and 0.01× those of cows). On average 58% of the animals at the dairies would need to be heifers for the bottom-up estimates to agree with the aircraft-derived fluxes. However, the large dairies targeted here generally keep only milking cows on-site, with heifers raised at separate facilities.

4 Conclusions and Implications

The aircraft-based constraints derived here support current bottom-up methane estimates for beef concentrated animal feeding operations (CAFOs), while pointing to a substantial current overestimate of emissions from sugar plants (plus a possible bias in the associated seasonality). Top-down results for dairies and swine CAFOs suggest that the factors driving variability in manure related emissions are not well-captured in current large-scale inventories used in models. While our present mechanistic understanding of these emissions is supported by many site-level studies [e.g. *Kariyapperuma et al.*, 2018; *Park et al.*, 2006; *Ulyatt et al.*, 2002], some key management variables are described in large-scale inventories using regional- or national-scale statistics that may not accurately reflect a particular measurement setting. Our results therefore do not necessarily indicate a bias in the magnitude of manure methane emissions, since emissions may have occurred preferentially at times or locations not captured by the aircraft (e.g., following lagoon cover removal or application to fields).

Two recent regional-to-national scale inverse modeling studies inferred a substantial underestimate in current methane emission estimates for animal agriculture [*Chen et al.*, 2018; *Miller et al.*, 2013]. If correct, that finding implies bottom-up biases either in the activity rates or in the methane EFs themselves. The point-source results here do not point to a persistent EF underestimate arguing against the latter explanation (though such biases may conceivably vary geographically between the study domains). To assess the potential role of activity biases, we compared our top-down point source fluxes with the total monthly methane emissions predicted for the surrounding $0.1^{\circ} \times 0.1^{\circ}$ grid cells in the Gridded EPA inventory [*Maasackers et al.*, 2016]. Indeed, the GEM aircraft-based fluxes (in kg/h) are on average $3.9\times$ the Gridded EPA emissions for those grid cells containing CAFOs, despite the fact that the former represents a single facility and the latter represents the entire surrounding $0.1^{\circ} \times 0.1^{\circ}$ land area. This disparity suggests errors in the magnitude or spatial allocation of livestock activity rates. Conversely, the aircraft-based fluxes are on average only $0.2\times$ the Gridded EPA emissions for grid cells containing sugar plants. Such spatial and temporal errors in bottom-up methane emission estimates will also affect the prior estimates used for inverse modeling, potentially leading to mis-categorization of sources. A possible step to reduce such biases is through more detailed spatial allocation of methane emissions from CAFOs [*Hedelius et al.*, 2018]. Recent studies [*Varon et al.*, 2018; 2019] have explored the possibility of using satellite data to quantify methane point sources, which, if anticipated performance targets are met, would offer the dual advantages of sustained temporal sampling and regional (or broader) spatial coverage. However, the estimated error is

approximately 100-300 kg/h for a 10×10 km² satellite footprint [Varon *et al.*, 2018], corresponding to an uncertainty of up to 360% for the median top-down fluxes calculated here. A combination of remote and in-situ techniques will therefore be needed to accurately quantify methane emissions across the full range of relevant facility sizes.

Acknowledgements and Data Availability Statement

We thank Jason Rosenthal, Justin Pifer, and Ian Locko for their excellent flying; Julian Deventer, Xiang Li, and Matt Erickson for assistance with instrument calibration; Kurt Spokas, Lisa Scheirer and David Weinand for the insightful suggestions. The GEM project is supported by NASA's Interdisciplinary Research in Earth Science program (IDS Grant #NNX17AK18G). XY acknowledges support from a NASA Earth and Space Science Fellowship (Grant #80NSSC18K1393). JDW acknowledges support from the US Department of Energy (DOE), Office of Science, Office of Biological and Environmental Research Program, through Oak Ridge National Laboratory's Terrestrial Ecosystem Science–Science Focus Area; ORNL is managed by UT-Battelle, LLC, for DOE under contract DE-AC05-00OR22725. Data presented in this paper is publicly available at <https://doi.org/10.13020/f50r-zh70>.

References

ACSC, American Crystal Sugar Company (2019), Retrieved on July 21, 2019, from <https://www.crystalsugar.com/sugar-processing/environmental-commitment/frequently-asked-questions/>.

Beauchemin, K., Kreuzer, M., O'mara, F., & McAllister, T. (2008), Nutritional management for enteric methane abatement: a review, *Australian Journal of Experimental Agriculture*, 48(2), 21-27.

Bloom, A. A., Bowman, K. W., Lee, M., Turner, A. J., Schroeder, R., Worden, J. R., et al. (2017), A global wetland methane emissions and uncertainty dataset for atmospheric chemical transport models (WetCHARTs version 1.0), *Geoscientific Model Development*, 10(6), 2141-2156.

Boadi, D., Benchaar, C., Chiquette, J., & Massé, D. (2004), Mitigation strategies to reduce enteric methane emissions from dairy cows: Update review, *Canadian Journal of Animal Science*, 84(3), 319-335.

Chen, Z., Griffis, T. J., Baker, J. M., Millet, D. B., Wood, J. D., Dlugokencky, E. J., et al. (2018), Source Partitioning of Methane Emissions and its Seasonality in the U.S. Midwest, *Journal of Geophysical Research: Biogeosciences*, 123(2), 646-659, doi:10.1002/2017JG004356.

Conley, S., Faloon, I., Mehrotra, S., Suard, M., Lenschow, D. H., Sweeney, C., et al. (2017), Application of Gauss's theorem to quantify localized surface emissions from airborne measurements of wind and trace gases, *Atmospheric Measurement Techniques*, 10(9), 3345-3358.

Cui, Y. Y., Brioude, J., Angevine, W. M., Peischl, J., McKeen, S. A., Kim, S., et al. (2017), Top-down estimate of methane emissions in California using a mesoscale inverse modeling technique:

The San Joaquin Valley, *Journal of Geophysical Research: Atmospheres*, 122(6), 3686-3699, doi:10.1002/2016JD026398.

Dilek, F. B., Yetis, U., & Gökçay, C. F. (2003), Water savings and sludge minimization in a beet-sugar factory through re-design of the wastewater treatment facility, *Journal of Cleaner Production*, 11(3), 327-331, doi:10.1016/S0959-6526(02)00029-X.

eCFR (2019), Electronic Code of Federal Regulations Subpart TT - Industrial Waste Landfills. Retrieved on January 31, 2019, from <https://www.ecfr.gov/cgi-bin/retrieveECFR?gp=&SID=e432fd268d29a719e9b083b1434fc3cf&mc=true&n=sp40.23.98.tt&r=SUBPART&ty=HTML>.

EDGAR, Emission Database for Global Atmospheric Research, v4.2 FT2010, 2013. <https://edgar.jrc.ec.europa.eu/overview.php?v=42FT2010>.

Gelaro, R., McCarty, W., Suárez, M. J., Todling, R., Molod, A., Takacs, L., et al. (2017), The modern-era retrospective analysis for research and applications, version 2 (MERRA-2), *Journal of Climate*, 30(14), 5419-5454.

GHGRP, Greenhouse Gas Reporting Program (2019). Retrieved on November 23, 2019, from <https://ghgdata.epa.gov/ghgp/main.do>.

Gvakharia, A., Kort, E. A., Brandt, A., Peischl, J., Ryerson, T. B., Schwarz, J. P., et al. (2017), Methane, black carbon, and ethane emissions from natural gas flares in the Bakken Shale, North Dakota, *Environmental Science & Technology*, 51(9), 5317-5325.

Gvakharia, A., Kort, E. A., Smith, M. L., & Conley, S. (2018), Testing and evaluation of a new airborne system for continuous N₂O, CO₂, CO, and H₂O measurements: the Frequent Calibration High-performance Airborne Observation System (FCHAOS), *Atmospheric Measurement Techniques*, 11(11), 6059-6074, doi:10.5194/amt-11-6059-2018.

Harun, S. M. R., & Ogneva-Himmelberger, Y. (2013), Distribution of Industrial Farms in the United States and Socioeconomic, Health, and Environmental Characteristics of Counties, *Geography Journal*, 2013, 12, doi:10.1155/2013/385893.

Hedelius, J. K., Liu, J., Oda, T., Maksyutov, S., Roehl, C. M., Iraci, L. T., et al. (2018), Southern California megacity CO₂, CH₄, and CO flux estimates using ground- and space-based remote sensing and a Lagrangian model, *Atmospheric Chemistry and Physics*, 18(22), 16271-16291, doi:10.5194/acp-18-16271-2018.

Hristov, A. N., Harper, M., Meinen, R., Day, R., Lopes, J., Ott, T., et al. (2017), Discrepancies and uncertainties in bottom-up gridded inventories of livestock methane emissions for the contiguous United States, *Environmental Science & Technology*, 51(23), 13668-13677.

Hristov, A. N., Johnson, K. A., & Kebreab, E. (2014), Livestock methane emissions in the United States, *Proceedings of the National Academy of Sciences*, 111(14), E1320-E1320, doi:10.1073/pnas.1401046111.

IADNR, Iowa Department of Natural Resources, Retrieved on June 14, 2018, from <https://programs.iowadnr.gov/animalfeedingoperations/Default.aspx>.

IPCC (2006), *2006 IPCC Guidelines for National Greenhouse Gas Inventories*. The National Greenhouse Gas Inventories Programme, The Intergovernmental Panel on Climate Change. H.S. Eggleston, L. Buendia, K. Miwa, T. Ngara, and K. Tanabe (eds.). Hayama, Kanagawa, Japan.

Johnson, M. R., Tyner, D. R., Conley, S., Schwietzke, S., & Zavala-Araiza, D. (2017), Comparisons of airborne measurements and inventory estimates of methane emissions in the Alberta upstream oil and gas sector, *Environmental Science & Technology*, *51*(21), 13008-13017.

Karion, A., Sweeney, C., Kort, E. A., Shepson, P. B., Brewer, A., Cambaliza, M., et al. (2015), Aircraft-Based estimate of total methane emissions from the Barnett Shale region, *Environmental Science & Technology*, *49*(13), 8124-8131, doi:10.1021/acs.est.5b00217.

Kariyapperuma, K. A., Johannesson, G., Maldaner, L., VanderZaag, A., Gordon, R., & Wagner-Riddle, C. (2018), Year-round methane emissions from liquid dairy manure in a cold climate reveal hysteretic pattern, *Agricultural and Forest Meteorology*, *258*, 56-65, doi:10.1016/j.agrformet.2017.12.185.

Krings, T., Neininger, B., Gerilowski, K., Krautwurst, S., Buchwitz, M., Burrows, J. P., et al. (2018), Airborne remote sensing and in situ measurements of atmospheric CO₂ to quantify point source emissions, *Atmospheric Measurement Techniques*, *11*(2), 721-739.

Lavoie, T. N., Shepson, P. B., Cambaliza, M. O., Stirm, B. H., Conley, S., Mehrotra, S., et al. (2017), Spatiotemporal variability of methane emissions at oil and natural gas operations in the Eagle Ford Basin, *Environmental Science & Technology*, *51*(14), 8001-8009.

Maasackers, J. D., Jacob, D. J., Sulprizio, M. P., Turner, A. J., Weitz, M., Wirth, T., et al. (2016), Gridded national inventory of U.S. methane emissions, *Environmental Science & Technology*, 50(23), 13123-13133, doi:10.1021/acs.est.6b02878.

Maldaner, L., Wagner-Riddle, C., VanderZaag, A. C., Gordon, R., & Duke, C. (2018), Methane emissions from storage of digestate at a dairy manure biogas facility, *Agricultural and Forest Meteorology*, 258, 96-107, doi: 10.1016/j.agrformet.2017.12.184.

Mehrotra, S., Faloona, I., Suard, M., Conley, S., & Fischer, M. L. (2017), Airborne methane emission measurements for selected oil and gas facilities across California, *Environmental Science & Technology*, 51(21), 12981-12987.

Miller, S. M., Michalak, A. M., & Wofsy, S. C. (2014), Reply to Hristov et al.: Linking methane emissions inventories with atmospheric observations, *Proceedings of the National Academy of Sciences*, 111(14), E1321-E1321, doi:10.1073/pnas.1401703111.

Miller, S. M., Wofsy, S. C., Michalak, A. M., Kort, E. A., Andrews, A. E., Biraud, S. C., et al. (2013), Anthropogenic emissions of methane in the United States, *Proceedings of the National Academy of Sciences*, 110(50), 20018-20022, doi:10.1073/pnas.1314392110.

Park, K.-H., Thompson, A. G., Marinier, M., Clark, K., & Wagner-Riddle, C. (2006), Greenhouse gas emissions from stored liquid swine manure in a cold climate, *Atmospheric Environment*, 40(4), 618-627.

Ryoo, J. M., Iraci, L. T., Tanaka, T., Marrero, J. E., Yates, E. L., Fung, I., et al. (2019), Quantification of CO₂ and CH₄ emissions over Sacramento, California, based on divergence theorem using aircraft measurements, *Atmospheric Measurement Techniques*, 12(5), 2949-2966, doi:10.5194/amt-12-2949-2019.

Scheutz, C., Kjeldsen, P., Bogner, J. E., De Visscher, A., Gebert, J., Hilger, H. A., et al. (2009), Microbial methane oxidation processes and technologies for mitigation of landfill gas emissions, *Waste Management & Research*, 27(5), 409-455.

SMBSC, Southern Minnesota Beet Sugar Cooperative (2019), Retrieved July 21, 2019, from <http://www.smbc.com/OurSugar/SugarProcess/WaterTreatment.aspx>.

Smith, M. L., Gvakharia, A., Kort, E. A., Sweeney, C., Conley, S. A., Faloon, I., et al. (2017), Airborne quantification of methane emissions over the four corners region, *Environmental Science & Technology*, 51(10), 5832-5837.

Turner, A. J., Jacob, D. J., Wecht, K. J., Maasakkers, J. D., Lundgren, E., Andrews, A. E., et al. (2015). Estimating global and North American methane emissions with high spatial resolution using GOSAT satellite data, *Atmospheric Chemistry and Physics*, 15 (12), 7049-7069.

Ulyatt, M. J., Lassey, K. R., Shelton, I. D., & Walker, C. F. (2002), Seasonal variation in methane emission from dairy cows and breeding ewes grazing ryegrass/white clover pasture in New Zealand, *New Zealand Journal of Agricultural Research*, 45(4), 217-226, doi:10.1080/00288233.2002.9513512.

USDA-NASS, United States Department of Agriculture, National Agricultural Statistics Service (2018). Retrieved on June 3, 2018, from <https://quickstats.nass.usda.gov>.

USEPA, U.S. Environmental Protection Agency (2018). Retrieved on April 18, 2018, from <https://www.epa.gov/ghgemissions/inventory-us-greenhouse-gas-emissions-and-sinks-1990-2014>.

USGS, US Geological Survey (2019), retrieved February 20, 2019, from <https://nationalmap.gov/elevation.html>.

VanderZaag, A., MacDonald, J., Evans, L., Vergé, X., & Desjardins, R. (2013), Towards an inventory of methane emissions from manure management that is responsive to changes on Canadian farms, *Environmental Research Letters*, 8(3), 035008, doi:10.1088/1748-9326/8/3/035008.

VanderZaag, A. C., Flesch, T. K., Desjardins, R. L., Baldé, H., & Wright, T. (2014), Measuring methane emissions from two dairy farms: Seasonal and manure-management effects, *Agricultural and Forest Meteorology*, 194, 259-267, doi:10.1016/j.agrformet.2014.02.003.

Varon, D. J., Jacob, D. J., McKeever, J., Jervis, D., Durak, B. O. A., Xia, Y., & Huang, Y. (2018), Quantifying methane point sources from fine-scale satellite observations of atmospheric methane plumes, *Atmospheric Measurement Techniques*, 11(10), 5673-5686, doi:10.5194/amt-11-5673-2018.

Varon, D. J., McKeever, J., Jervis, D., Maasackers, J. D., Pandey, S., Houweling, S., et al. (2019). Satellite discovery of anomalously large methane point sources from oil/gas production. *Geophysical Research Letters*, 46. doi:10.1029/2019GL083798.

Vaughn, T. L., Bell, C. S., Yacovitch, T. I., Roscioli, J. R., Herndon, S. C., Conley, S., et al. (2017), Comparing facility-level methane emission rate estimates at natural gas gathering and boosting stations, *Elementa: Science of the Anthropocene*, 5(17). doi:10.1525/elementa.257.

Table 1. Point Sources Quantified by GEM Flights

| Type | Facility ID | Herd Size ¹ (head) | Season | Top-down Emissions (kg/h) | Top-down Uncertainty Range ² (kg/h) | Bottom-up Emissions (kg/h) | Bottom-up Uncertainty Range ³ (kg/h) |
|-------------|---------------|----------------------------------|--------|------------------------------|---|-------------------------------|--|
| Dairy | Dairy A | 8,000 | Summer | 98 | [53, 144] | 221 | [170, 277] |
| | | | Winter | 118 | [96, 139] | 166 | [106, 218] |
| | | | Spring | 171 | [146, 202] | 226 | [170, 285] |
| | Dairy B | 7,000 | Summer | 28 | [11, 120] | 193 | [149, 242] |
| | | | Winter | 78 | [64, 89] | 145 | [93, 190] |
| | | | Spring | 108 | [72, 143] | 189 | [149, 233] |
| | Dairy C | 6,500 | Summer | 26 | [23, 32] | 179 | [138, 225] |
| | | | Winter | 130 | [113, 145] | 135 | [86, 177] |
| | | | Spring | 77 | [47, 107] | 176 | [138, 217] |
| | Dairy D | 6,500 | Summer | 78 | [61, 95] | 179 | [138, 224] |
| | | | Winter | 132 | [105, 148] | 135 | [87, 177] |
| | | | Spring | 91 | [63, 113] | 183 | [138, 231] |
| Dairy E | 6,000 | Winter | 82 | [55, 98] | 124 | [80, 163] | |
| | | Spring | 124 | [90, 160] | 170 | [127, 214] | |
| Beef CAFO | Beef CAFO A | 11,925 | Winter | 53 | [40, 65] | 70 | [55, 85] |
| | | | Spring | 74 | [63, 83] | 72 | [58, 86] |
| | Beef CAFO B | 10,500 | Summer | 26 | [-13, 76] | 61 | [48, 73] |
| | | | Winter | 38 | [19, 64] | 58 | [46, 71] |
| Swine CAFO | Swine CAFO A | 20,080 | Spring | 162 | [143, 182] | 67 | [39, 70] |
| | Swine CAFO B | 28,588 | Spring | 6 | [-12, 37] | 78 | [51, 87] |
| Sugar Plant | Sugar Plant A | | Summer | 146 | [128, 160] | 473 | [464, 622] |
| | | | Winter | 38 | [-11, 96] | 471 | [463, 620] |
| | | | Spring | 161 | [126, 198] | 471 | [463, 620] |
| | Sugar Plant B | | Winter | 41 | [31, 53] | 569 | [424, 574] |

¹On-site animal population (see text for details).

²Top-down uncertainty ranges include contributions from meteorological factors, instrument error, and sampling lag as discussed in-text.

³Bottom-up uncertainty ranges for dairies and concentrated animal feeding operations (CAFOs) include contributions from enteric fermentation and manure emissions as described in-text.

Figure 1. GEM flight tracks and point source locations. Flight tracks are colored according to the observed methane mixing ratios (2-min average). Annual wetland methane emissions from the WetCHARTs inventory [Bloom *et al.*, 2017] are shown in the left panel, annual livestock emissions from the Gridded EPA inventory [Maasakkers *et al.*, 2016] are shown in the middle panel, and annual other anthropogenic emissions [Maasakkers *et al.*, 2016] are shown in the right panel. Detailed information for each point source is provided in Tables 1 and S1.

Figure 2. Illustration of the aircraft-based point source quantification approach, showing the flight direction (s) along with the heights of interpolated layers (Δz_j) and of the surface layer (Δz_1). Also shown are the vertical methane profiles for upwind and downwind sectors (Dairy D; 01/28/2018). Points indicate individual methane observations while the bars show the range in observed methane for each layer. Facility is not drawn to scale. For details, see text and supporting information.

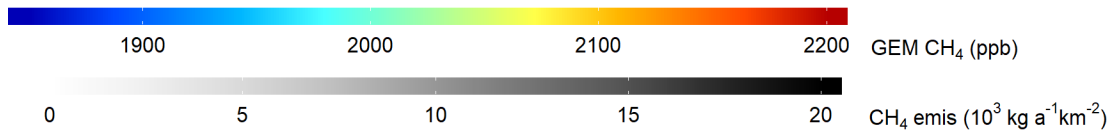
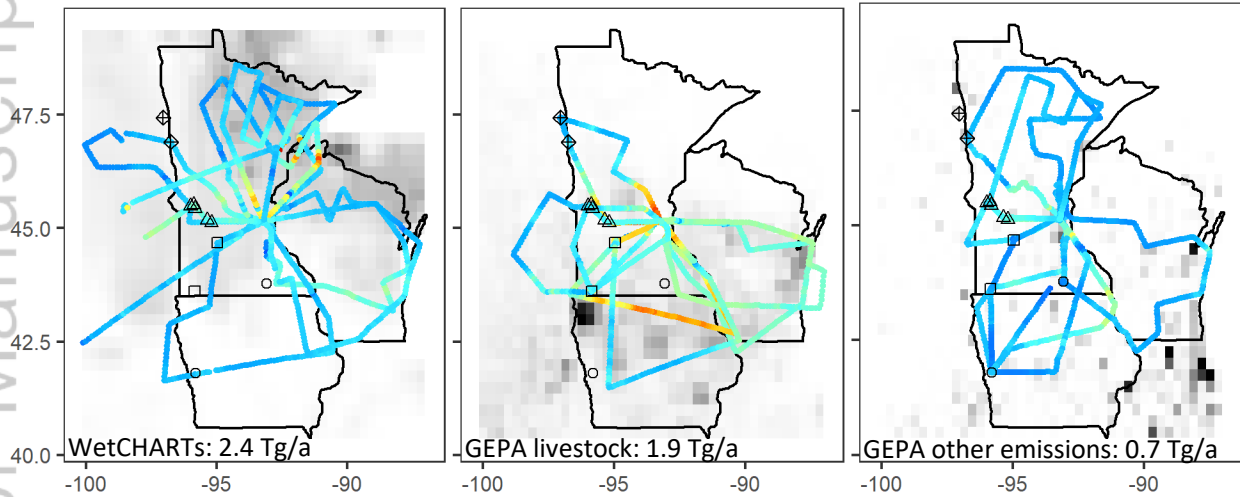
Figure 3. Aircraft-based versus bottom-up methane point source emission estimates. Aircraft-based best estimates are shown as red circles (error bars indicate the associated uncertainty). Red pluses show results from individual site visits. Bottom-up best-estimate emissions are shown as black lines, with gray shading indicating the uncertainty range. Panels a-i show results for dairies, beef and swine concentrated animal feeding operations (CAFOs), which include bottom-up contributions from manure management (blue lines with uncertainty shown as light blue shading, see text for details) and enteric fermentation (green lines and shading). Panels j-k show sugar

processing facility results, with >99% of the bottom-up methane flux from waste/landfill emissions. See text for details.

GEM1 - Summer (2017 Aug.)

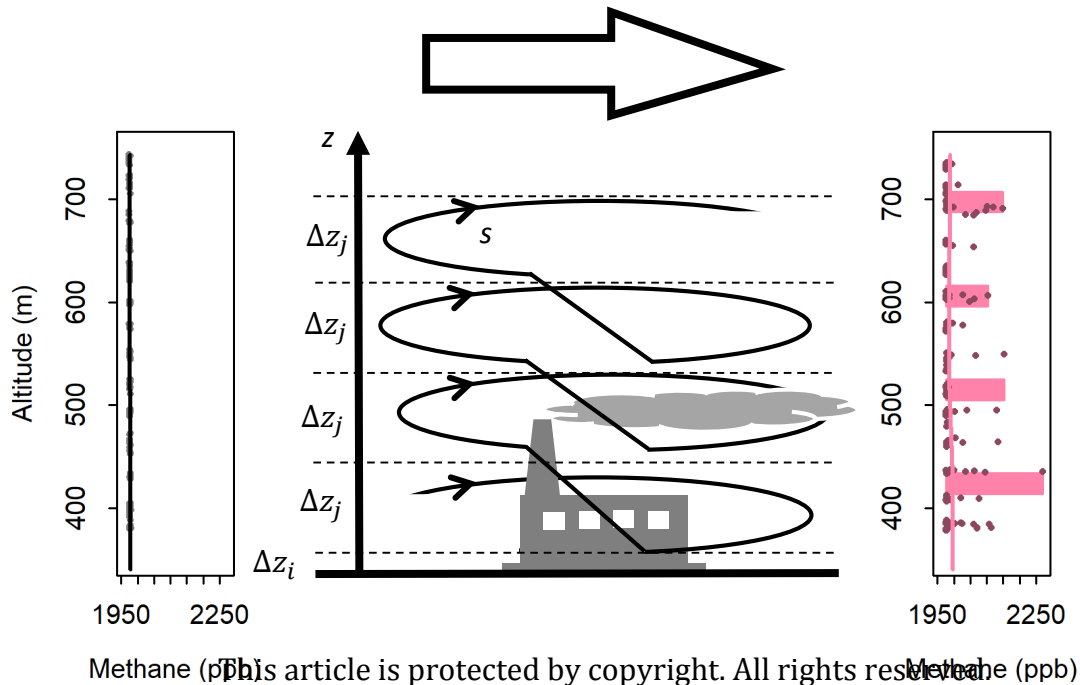
GEM2 - Winter (2018 Jan.)

GEM3 - Spring (2018 May-Jun.)



This article is protected by copyright. All rights reserved.

⊕ sugar □ beef △ dairy ○ swine



This article is protected by copyright. All rights reserved.

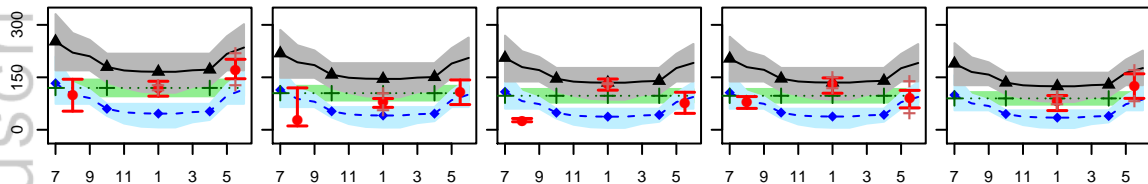
a) Dairy A

b) Dairy B

c) Dairy C

d) Dairy D

e) Dairy E



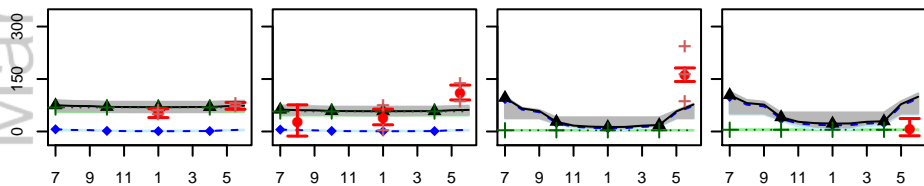
f) Beef CAFO A

g) Beef CAFO B

h) Swine CAFO A

i) Swine CAFO B

Emission (kg/hr)



Aircraft-Based Estimate

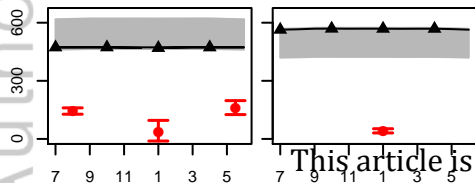
- Best Estimate
- + Site Visit

Bottom-Up Emissions

- ▲ Total
- ◆ Manure
- ◆ Enteric

j) Sugar Plant A

k) Sugar Plant B



Aircraft-Based Estimate

- Best Estimate

Bottom-Up Emissions

- ▲ Total

This article is protected by copyright. All rights reserved.

Month (07/2017 – 06/2018)